Physics Letters B 761 (2016) 412–418

Contents lists available at ScienceDirect

Physics Letters B

www.elsevier.com/locate/physletb

Interaction cross section study of the two-neutron halo nucleus ^{22}C

Y. Togano [a,*], T. Nakamura [a], Y. Kondo [a], J.A. Tostevin [b], A.T. Saito [a], J. Gibelin [c], N.A. Orr [c], N.L. Achouri [c], T. Aumann [d], H. Baba [e], F. Delaunay [c], P. Doornenbal [e], N. Fukuda [e], J.W. Hwang [f], N. Inabe [e], T. Isobe [e], D. Kameda [e], D. Kanno [a], S. Kim [f], N. Kobayashi [a], T. Kobayashi [g], T. Kubo [e], S. Leblond [c], J. Lee [e], F.M. Marqués [c], R. Minakata [a], T. Motobayashi [e], D. Murai [h], T. Murakami [i], K. Muto [g], T. Nakashima [a], N. Nakatsuka [i], A. Navin [j], S. Nishi [a], S. Ogoshi [a], H. Otsu [e], H. Sato [e], Y. Satou [f], Y. Shimizu [e], H. Suzuki [e], K. Takahashi [g], H. Takeda [e], S. Takeuchi [e], R. Tanaka [a], A.G. Tuff [k], M. Vandebrouck [l], K. Yoneda [e]

[a] Department of Physics, Tokyo Institute of Technology, Tokyo 152-8551, Japan
[b] Department of Physics, Faculty of Engineering and Physical Sciences, University of Surrey, GU2 7XH, United Kingdom
[c] LPC Caen, ENSICAEN, Université de Caen, CNRS/IN2P3, 14050 Caen Cedex, France
[d] Institut für Kernphysik, Technische Universität Darmstadt, D-64289 Darmstadt, Germany
[e] RIKEN Nishina Center, Saitama 351-0198, Japan
[f] Department of Physics and Astronomy, Seoul National University, 599 Gwanak, Seoul 151-742, Republic of Korea
[g] Department of Physics, Tohoku University, Miyagi 980-8578, Japan
[h] Department of Physics, Rikkyo University, Tokyo 171-8501, Japan
[i] Department of Physics, Kyoto University, Kyoto 606-8502, Japan
[j] GANIL, CEA/DSM-CNRS/IN2P3, F-14076 Caen Cedex 5, France
[k] Department of Physics, University of York, Heslington, York YO10 5DD, United Kingdom
[l] IPN Orsay, Université Paris Sud, IN2P3-CNRS, F-91406 Orsay Cedex, France

ARTICLE INFO

Article history:
Received 29 December 2015
Received in revised form 4 August 2016
Accepted 30 August 2016
Available online 1 September 2016
Editor: V. Metag

Keywords:
Interaction cross section
Matter radius
Two-neutron halo nucleus ^{22}C

ABSTRACT

The interaction cross sections (σ_I) of the very neutron-rich carbon isotopes ^{19}C, ^{20}C and ^{22}C have been measured on a carbon target at 307, 280, and 235 MeV/nucleon, respectively. A σ_I of 1.280 ± 0.023 b was obtained for ^{22}C, significantly larger than for ^{19,20}C, supporting the halo character of ^{22}C. A ^{22}C root-mean-squared matter radius of 3.44 ± 0.08 fm was deduced using a four-body Glauber reaction model. This value is smaller than an earlier estimate (of 5.4 ± 0.9 fm) derived from a σ_I measurement on a hydrogen target at 40 MeV/nucleon. These new, higher-precision σ_I data provide stronger constraints for assessing the consistency of theories describing weakly bound nuclei.

The nuclear halo, a valence neutron distribution that extends far beyond a well-bound core, is a characteristic feature of very weakly bound nuclei far from stability [1]. Borromean two-neutron halo systems, such as ^{11}Li, are of particular interest for the study of many-body effects, such as possible strong neutron–neutron (nn) correlations [2–11]. In the case of ^{11}Li, the analysis of interaction cross section data using simplified reaction and structure models was sufficient to identify a large difference between the root-mean-squared (rms) radii, $\tilde{r}_m$, of ^{11}Li ($3.34^{+0.04}_{-0.08}$ fm) and ^{9}Li (2.32 ± 0.02 fm) [12–14]. It is known however that dynamical models that include breakup degrees of freedom are necessary for accurate quantitative analyses, and that these increase the deduced $\tilde{r}_m$ values for halo systems [15,16].

Recently, the most neutron-rich bound carbon isotope ^{22}C (two-neutron separation energy $S_{2n} = -0.14 \pm 0.46$ MeV [17]) has drawn considerable attention, owing to a possibly very-extended two-neutron halo structure – as suggested by a large reaction cross section ($\sigma_R = 1.338 \pm 0.274$ b) measured on a proton target at 40 MeV/nucleon [18]. An associated $\tilde{r}_m$ of 5.4 ± 0.9 fm, with relatively large uncertainty, was deduced. This value is significantly

* Corresponding author.
E-mail address: togano@phys.titech.ac.jp (Y. Togano).

http://dx.doi.org/10.1016/j.physletb.2016.08.062

larger than that for well-known halo nuclei such as ^{11}Li. The nucleus ^{22}C is also significant in terms of magicity at $N = 16$, as was recently established for ^{24}O [19–21]. Clarifying whether $N = 16$ magicity persists in ^{22}C will shed light on the shell evolution along the neutron drip-line. Importantly, if the $N = 16$ shell closure in ^{22}C is confirmed, the two-neutron valence configuration would be $[2s_{1/2}]^2$, optimal for halo formation. The structure of ^{22}C may also provide some clues as to why the drip line ends at $N = 16$ in the carbon, nitrogen, and oxygen isotopes. Experimentally, evidence for $N = 16$ magicity has been found in the two-neutron removal cross section from ^{22}C and the resulting ^{20}C fragment momentum distribution [22].

The large uncertainties on the earlier measurement of σ_R and the deduced $\tilde{r}_m$ [18] do not significantly constrain the theoretical models. A mean-field approach, using an adjusted Skyrme interaction, predicted $\tilde{r}_m$ of 3.89 fm [23]. Three-body model calculations for ^{22}C, with dominant $[2s_{1/2}]^2$ valence neutron configurations [24,25], derive $\tilde{r}_m$ in the range 3.50–3.70 fm. Given the increased mass of ^{22}C, and the resulting smaller fractional contribution of the two valence nucleons to $\tilde{r}_m$, all three-body model calculations [24–27] require extremely weak two-valence-neutron binding to produce an enhanced $\tilde{r}_m$. Given the significant error on the experimental estimate of Ref. [18] and that the theoretical values are within $\sim 2\sigma$ of this value, more definitive conclusions require data of significantly higher precision.

In this spirit, the present Letter reports a high precision ^{22}C interaction cross section (σ_I) measurement on a carbon target at 235 MeV/nucleon. At this energy, unlike the earlier 40 MeV/nucleon proton target measurement, the assumed forward scattering dominance of the core and valence particles, that underpins the Glauber (eikonal) model description, is well satisfied. In addition, it has been shown that the optical limit (OL) approximation to Glauber theory provides an excellent description of the (reasonably well-bound) core-target systems without the need to consider additional (Fermi-motion [28] and Pauli blocking [29]) corrections – a result of the highly absorptive nature of the core-target interactions in the case of a light nuclear (carbon) target.

There remains, however, a small uncertainty due to the difference between σ_I, derived from the measurement, and the reaction cross section σ_R that is typically calculated using the Glauber model analysis. As measured, σ_I is the cross section for a change of nuclide in the collision [30] while $\sigma_R = \sigma_I + \sigma_{inel}$ also includes any inelastic cross section to bound excited states of the projectile and target. Since σ_{inel} is small at the present beam energy, as will be shown later, σ_I is a very good approximation to σ_R with the present experimental (energy and target) conditions.

Here, the ^{19,20,22}C projectile systems will be treated in a consistent framework where: (i) the relatively well-bound (non-halo) core nuclei, ^{18,20}C, are described using Hartree–Fock (HF) densities in which the least-bound orbitals are constrained to the empirical neutron separation energies, and (ii) the structure and dynamics of the weakly-bound valence neutron degrees of freedom in the halo-systems ^{19,22}C are treated explicitly using few-body methods. So, three- and four-body Glauber model descriptions are used for the ^{19}C and ^{22}C-target systems, respectively. The $\tilde{r}_m$ of ^{22}C is thus derived from σ_R by comparisons with four-body Glauber reaction model calculations (see e.g. [15,16]) that incorporate three-body model ^{22}C ground-state wave functions. Comparisons with the measured σ_R for ^{20}C (the ^{22}C core) and the one-neutron halo nucleus ^{19}C are used to assess the consistency of this approach.

The experiment was performed at the Radioactive Isotope Beam Factory (RIBF) accelerator complex operated by the RIKEN Nishina Center and Center for Nuclear Study, University of Tokyo. A cocktail beam of ^{19,20,22}C was produced via projectile fragmentation of a 345 MeV/nucleon ^{48}Ca beam from the Superconducting Ring

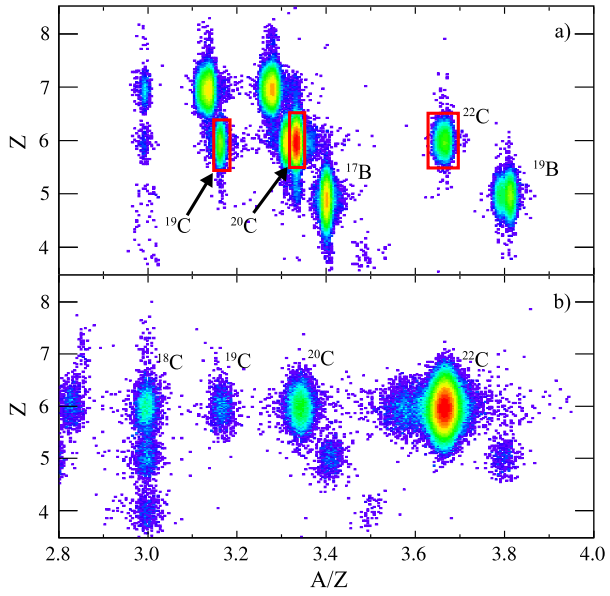

Fig. 1. (Color online.) Particle-identification plots of a) the secondary beam and b) outgoing reaction products from ^{22}C. The color scale is logarithmic. The red squares in a) show the condition used for the analyses.

Cyclotron incident on a 20 mm thick Be target. The ^{19,20,22}C fragments were separated using the BigRIPS [31] with an aluminum degrader with a medium thickness of 15 mm placed at the first dispersive focal plane. The momentum acceptance was set to be ±3%. The cocktail beam impinged on a carbon target with a thickness of 1.789 g/cm^2. The typical ^{19,20,22}C intensities were 6.0, 290, and 6.6 Hz, respectively, which corresponded to approximately 0.36%, 18%, and 0.41% of the total secondary beam intensity. The mean energies of the ^{19,20,22}C beams at the target mid-point were 307, 280, 235 MeV/nucleon, respectively.

The secondary beam particles were monitored event-by-event using two multi-wire drift chambers (BDC [32]) placed just upstream of the carbon target, in order to ascertain the incident angle and position upon the target. The incident particles were identified by measuring the time-of-flight (TOF), magnetic rigidity ($B\rho$), and energy loss (ΔE) with plastic scintillators, a multi-wire proportional counter, and an ionization chamber upstream of the carbon target. Fig. 1a) shows the atomic number (Z) and the mass to charge ratio (A/Z) reconstructed from the measured $B\rho$, TOF and ΔE. A small fraction of events were observed that are shifted slightly to a smaller A/Z for ^{20}C. These events were found to follow a different trajectory from the main one, and were mostly removed. Nevertheless, we still had such unwanted beam particles of about 0.03% of the respective isotope. Hence, by selecting the isotopes as shown in Fig. 1a), such events are not used in the analysis. Contamination from $Z = 7$ particles in the gated region of ^{19,20}C is found to be less than 6×10^{-6} of the selected events, which contributes negligibly (< 1 mb) to the current σ_I results. The target was surrounded by the DALI2 array [33] to detect de-excitation γ rays from excited outgoing fragments, which were used to estimate σ_{inel} as shown later.

The residues from the ^{19,20,22}C + C reactions were characterized using detectors located at the entrance and exit of the SAMURAI magnet – the detailed detector setup can be found in Ref. [32]. The $B\rho$ values of the charged particles were reconstructed using the positions and angles at two multi-wire drift chambers FDC1 and FDC2 [32]. The TOF was derived from the plastic scintillator hodoscope HODF located downstream of FDC2 with respect to the plastic scintillator (SBT) upstream of the carbon target. The ΔE

Table 1
Beam energies (at mid-target) and measured interaction cross sections (σ_I) for the carbon isotopes studied here. The two errors shown on σ_I are the statistical (first) and systematic (second) uncertainties.

A	E/A [MeV/nucleon]	σ_I [barn]
19	307	$1.125 \pm 0.025 \pm 0.013$
20	280	$1.111 \pm 0.008 \pm 0.009$
22	235	$1.280 \pm 0.022 \pm 0.007$

measured using FDC1 was also employed for the identification. Fig. 1b) shows the particle identification for the products from the ^{22}C + C reaction.

The interaction cross sections σ_I were derived using the conventional transmission method [30], where σ_I can be written as,

$$\sigma_I = -\frac{1}{N_t} \log\left(\frac{\Gamma}{\Gamma_0}\right). \quad (1)$$

Here, N_t is the number of target nuclei per unit area, while Γ is the ratio of the number of non-interacting outgoing particles to the number of incoming particles. Γ_0 corresponds to Γ for an empty target, to take into account reactions in the detectors [34]. The value of Γ_0 was determined to be ~ 0.98, while Γ was 0.87–0.89. The angular acceptance for the ejectiles was ± 2.9 degree in the vertical direction and ± 9.8 degree in the horizontal direction, which was sufficient to accept the non-reacted beams, given the beam spread of 0.5 degrees (FWHM) and the multiple scattering of 0.15 degrees (1σ) in the carbon target. The position on the target and incident angles of the ^{19,20,22}C beams were used to restrict the emittance so as to guarantee the full acceptance of the SAMURAI setup.

In the following discussion σ_I and σ_R are compared directly and it is assumed that the total inelastic scattering cross section, σ_{inel}, to the bound excited states in the projectile and target is negligible compared to σ_I. This assumption will be quantified and validated for the 280 MeV/nucleon ^{20}C + C data.

Table 1 presents the measured σ_I for ^{19,20,22}C with the statistical and systematic uncertainties. The systematic error is mainly governed by the variation of the detection efficiency of FDC2 between the C target and the empty target runs, since the hit position of the particles on FDC2 was different owing to the different $B\rho$ of the particles after the energy loss in the target. As is clear from Table 1, the σ_I value for ^{22}C is significantly enhanced relative to those of ^{19,20}C, consistent with a two-neutron halo character of ^{22}C.

The assumption that $\sigma_R \simeq \sigma_I$ is examined using the γ rays emitted in the ^{20}C + C $\rightarrow$ ^{20}C + X reaction. The γ-ray energy spectra, measured by DALI2 in coincidence with outgoing ^{20}C ions, are shown in Fig. 2. The upper and lower panels show the spectra in the laboratory and projectile frames, respectively. The red solid and black dashed curves show fits to the spectra and the components of the fit, respectively. In the laboratory frame, a peak at 4.4 MeV (with accompanying single- and double-escape peaks) is observed from the de-excitation of the ^{12}C(2_1^+) state of the target [35]. The peaks are fitted using Gaussian lineshapes and an exponential background and the cross section is, subsequently, deduced. The full energy peak efficiency is estimated using a Monte-Carlo simulation based on the GEANT4. The ^{12}C inelastic cross section is estimated to be ~ 4 mb. In the projectile frame, Fig. 2b), a peak at 1.6 MeV is clearly seen from the de-excitation of the known ^{20}C(2_1^+) state [36,37]. Fitting the peak with a Gaussian lineshape and an exponential background, the ^{20}C inelastic cross section is estimated to be ~ 3 mb. Importantly, the sum of the target and projectile inelastic cross sections is smaller than the uncertainty on the present ^{20}C interaction cross section. Such a small σ_{inel} is consistent with those deduced for the neutron-rich Mg isotopes at around 250 MeV/nucleon, obtained using a different analysis method [38]. The σ_{inel} for ^{19,22}C are expected to be smaller than for ^{20}C since ^{19,22}C are much more weakly bound. Having demonstrated the validity of comparing σ_R with σ_I, we now turn to the interpretation of the present results.

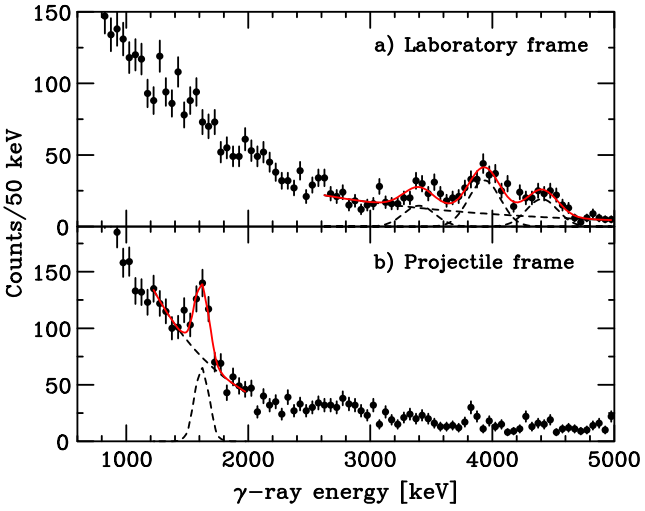

Fig. 2. (Color online.) The γ-ray energy spectrum in: a) the target frame, and b) the projectile frame, coincident with incoming ^{20}C and outgoing ^{20}C ions. In the target frame, the 4.4 MeV peak originates from the ^{12}C 2_1^+ state (see text). The projectile frame peak at 1.6 MeV originates from the ^{20}C 2_1^+ state.

To describe the reactions of the one- and two-neutron halo nuclei ^{19}C and ^{22}C three- and four-body Glauber dynamical models [15,16,25] are employed. For the relatively well-bound, non-halo projectile and ^{22}C core nucleus ^{20}C, the ^{19}C core nucleus ^{18}C, and ^{12}C (used as a test) we describe the collisions using the two-body optical limit (OL) Glauber model, based on the projectile/core-target S-matrices. The OL approach takes only the leading term in the ion–ion multiple scattering expansion and neglects correlations among the nucleons, other than the spatial correlations contained in the ground-state densities. Thus, in all of the subsequent reaction calculations, the n- and core-target interactions at the relevant beam energy are calculated consistently using the single-folding ($t_{NN}\rho_t$, n-target) and double-folding ($t_{NN}\rho_c\rho_t$, core-target) models, using an effective nucleon–nucleon (NN) interaction t_{NN}. The core (c) densities are taken from spherical Skyrme (SkX interaction [41]) Hartree–Fock (HF) calculations. The density of the carbon target nuclei was assumed to be Gaussian with an rms radius of 2.32 fm, consistent with the empirical rms charge radius [14]. Regarding the effective NN interaction, t_{NN} was assumed to be zero-range. Its (complex) strength, at each beam energy, was determined from: (i) the free NN cross sections, and (ii) the ratio of the real-to-imaginary parts of the NN forward scattering amplitude interpolated from the tabulated values of Ray [42]. We note that these folded n- and core-target interactions provide an excellent description of the recent n-removal data from the same neutron-rich carbon isotopes at 250 MeV/nucleon [22].

A partial assessment of the quality of this calculational scheme can be made using the previously measured energy dependence of the reaction cross sections for ^{12}C + ^{12}C [28,39,40]. The current OL Glauber calculations (blue curve) are compared with the available data in Fig. 3a) and show reasonable agreement above 200 MeV/nucleon.

The present reaction calculations for ^{19}C and ^{20}C are compared with the current and previous measurements in Figs. 3b) and c), respectively. The filled red circles and open diamond symbols show the present (~300 MeV/nucleon) and the previous

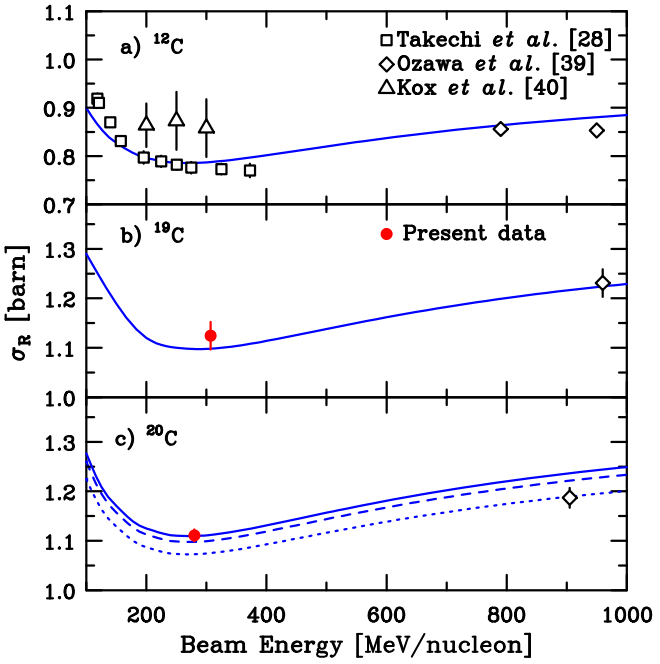

Fig. 3. (Color online.) Energy dependence of the reaction cross sections for (a) ^{12}C, (b) ^{19}C, and (c) ^{20}C on a ^{12}C target. The open diamonds, squares and triangles in (a) show the $^{12}C+^{12}C$ data from previous studies of Refs. [28,39,40], respectively. The filled red circles show the present results. The errors shown are the quadratic sum of the statistical and systematic uncertainties (Table 1). The blue curves in panels (b) and (c) are calculated using three-body and two-body Glauber models, respectively. Details are given in the text.

(∼900 MeV/nucleon) data [39]. The curve in Fig. 3b) shows the calculated energy dependence of σ_R for the ^{19}C + C system, using the three-body Glauber model of Refs. [15,16]. The model is consistent with the data points. We note that this calculation is essentially parameter free. The ^{19}C system is treated as a bound, $2s_{1/2}$, $^{18}C + n$ halo with the empirical neutron separation energy $S_n(^{19}C) = 0.58(9)$ MeV [43]. In constructing the HF density of the ^{18}C core, the $1d_{5/2}$ orbital is constrained to the known $S_n(^{18}C) = 4.180$ MeV, giving $\tilde{r}_m(^{18}C) = 2.75$ fm. So, combining the rms radii of the s-wave neutron wave function and the ^{18}C core [44], we obtain $\tilde{r}_m(^{19}C) = 3.10^{+0.05}_{-0.03}$ fm, where the uncertainty originates from the error on $S_n(^{19}C)$.

For ^{20}C, the present OL calculation results are presented in Fig. 3c). Both shell-model calculations of the $\langle^{19}C|^{20}C\rangle$ ground-state to ground-state overlap and the significant $^{19}C(1/2^+)$ ground-state yield measured in the neutron removal reaction from ^{20}C [22] indicate a significant occupancy of the $2s_{1/2}$ orbital in the ^{20}C ground-state. The calculated neutron $2s_{1/2}$ orbital occupancy of the ^{20}C ground-state (WBP) shell-model wave function, as used in Ref. [22], is 1.18. In computing the ^{20}C density for the OL calculations we thus constrain the HF calculations assuming a range of neutron $2s_{1/2}$ orbital occupancies to assess the sensitivity of the model to admixtures of this configuration. The $1d_{5/2}$ and $2s_{1/2}$ orbitals are assumed bound by $S_n(^{20}C) = 2.93$ MeV [43]. Fig. 3c) shows results with a $2s_{1/2}$ orbital occupancy of 0 (dotted), 1.2 (dashed) and 1.7 (solid). The results for $2s_{1/2}$ orbital occupancies between 1.2 and 1.7 are consistent with the present, high precision data point, whereas the earlier, higher-energy data point favours values at the lower end of this range. The $\tilde{r}_m(^{20}C)$ value of the HF density distribution with neutron $2s_{1/2}$ orbital occupancy of 1.2, the best fit to the both present and the high-energy data, is 2.95 ± 0.02 fm. The best fit to the present data using the HF, OL model, the solid curve, is $\tilde{r}_m(^{20}C) = 2.97^{+0.03}_{-0.05}$ fm, having a $2s_{1/2}$ orbital occupancy of $1.7^{+0.3}_{-0.8}$. The associated errors for $\tilde{r}_m$ and the $2s_{1/2}$ orbital occupancy arise from the uncertainty in the present reaction cross section and the known $S_n(^{20}C)$ of 2.93 ± 0.26 MeV. This result, $2.97^{+0.03}_{-0.05}$ fm, is adopted as the present result of $\tilde{r}_m(^{20}C)$. The reason why the calculated energy dependence of the solid curve, which best reproduces the current data point, overestimates the earlier higher energy data point is currently unclear. However, we note a similar trend in the $^{12}C+^{12}C$ system and data for the boron isotopes [45] and the source of this difference should be investigated further. We also note that the $\tilde{r}_m$ value extracted from Ref. [39], within an alternative framework, was (2.98 ± 0.05 fm), in excellent agreement with the current result. This is indicative that the reaction cross section measurement, in isolation, has insufficient sensitivity to accurately determine this occupancy, however the deduced $\tilde{r}_m$ value appears to be robustly determined.

For the ^{22}C + C system, we use a four-body (three-body projectile plus target) Glauber reaction model analysis [15,16], previously applied to ^{22}C. Full details of the physical inputs and the construction of the three-body model ^{22}C ground-state wave functions can be found in Ref. [25]. In these calculations [25], the additional pair of valence neutrons in ^{22}C are found to occupy the $2s_{1/2}$ orbital, with minimal $1d_{3/2}$ orbital occupancy. So, unlike the discussion above of the $2s_{1/2}$ occupancy of the free ^{20}C nucleus, in ^{22}C the valence nucleons essentially block access to the $2s_{1/2}$ orbital of nucleons from the ^{20}C core; consistent with the core having a filled $1d_{5/2}$ sub-shell. With the $1d_{5/2}$ orbital bound by $S_n(^{20}C) = 2.93$ MeV the HF ^{20}C core rms radius (in ^{22}C) is then 2.89 fm. This value is used when computing $\tilde{r}_m(^{22}C)$.

Solutions of the ^{22}C three-body wave functions use the Gogny, Pires and De Tourreil (GPT) nn interaction. The n–^{20}C interactions are described by Woods–Saxon potentials with a spin–orbit term. The parameters of these potentials in the $2s_{1/2}$ and $1d_{5/2,3/2}$ orbitals can be found in Ref. [25]. To provide a family of ^{22}C three-body wave functions with different ground-state eigenstates (i.e. binding energies E_{3B} $(= -S_{2n})$) and hence different sizes (rms hyperradii) we use a family of three-body Hamiltonians. These Hamiltonians differ in the choice of (i) the (unbound) $2s_{1/2}$ state potential depth (and their s-wave n–^{20}C scattering length) and (ii) the strength V_{3B} of the added attractive central hyperradial three-body force, $V_{3B}(\varrho) = -V_{3B}/(1 + [\varrho/5]^3)$, where ϱ is the hyperradius. Having fixed the Hamiltonian by choosing the above interaction strengths, the three-body wave function, its $\tilde{r}_m$, and $S_{2n}(^{22}C)$ are determined from the lowest eigenstate of the eigenvalue problem. The present results differ from those of Ref. [25] due to: (a) the incident beam energy, and (b) the use of the $S_n(^{20}C)$-constrained HF core density with $\tilde{r}_m(^{20}C(\text{core})) = 2.89$ fm, as was discussed above.

Fig. 4 shows, as filled squares, the dependence of the four-body Glauber calculations of σ_R on the $\tilde{r}_m(^{22}C)$ of the computed three-body ground-state wave functions. The points $k1$–$k5$ correspond to the wave functions of the same name tabulated in Table I of Ref. [25]. The remaining symbols extend this wave function set for more bound ^{22}C systems, with smaller $\tilde{r}_m(^{22}C)$, from 3.50 to 3.34 fm, by use of a more attractive three-body term, with V_{3B} values of 1.5, 1.8, 2.0, 2.5, 3.0 and 3.5 MeV. The symbols lie approximately on a straight line, showing that the calculated σ_R's are strongly sensitive to $\tilde{r}_m$ (and/or S_{2n}) but not to the finer details of the model interactions. The S_{2n} values of these wave functions range from 0.893–0.046 MeV as one moves from left to right in Fig. 4. All of the wave functions have dominant (92–94%) $[2s_{1/2}]^2$ and smaller (2–4%) $[1d_{3/2}]^2$ two-neutron configurations. The solid curve through the calculated results is a second order polynomial fit while the dashed horizontal line and the shaded region correspond to the measured value and 1σ error on σ_R from the present

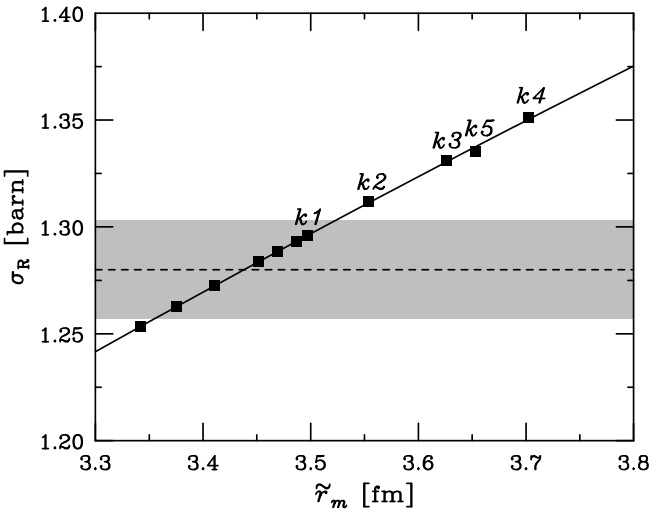

Fig. 4. Dependence of the calculated σ_R on the rms matter radius $\tilde{r}_m(^{22}\mathrm{C})$ within the four-body Glauber model. The filled squares are calculated results from the family of ^{22}C three-body wave functions. The solid curve is a second order polynomial fit to the calculations and the dashed line and the shaded region correspond to the measured value and 1σ error on σ_R deduced from the present experiment.

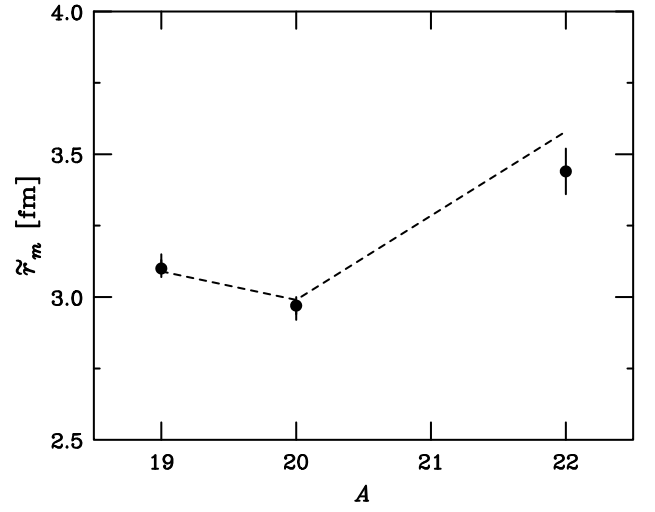

Fig. 5. Mass number dependence of the root-mean-squared radii of carbon isotopes obtained in the present study (filled circles). The dashed line connects the theoretical predictions of Ref. [46].

experiment, respectively. The error shown is the quadratic sum of the statistical and systematic uncertainties. From the model calculations of the figure we can estimate $\tilde{r}_m(^{22}\mathrm{C})$ and $S_{2n}(^{22}\mathrm{C})$ from the present data of 3.44 ± 0.08 fm and $0.56^{+0.27}_{-0.20}$ MeV, respectively. The $S_{2n}(^{22}\mathrm{C})$ value is consistent with the upper limit of 0.32 MeV from the direct mass measurement [17].

Consistent with our earlier discussion, this deduced $\tilde{r}_m(^{22}\mathrm{C})$ from the present few-body-model analysis is smaller, by about 2σ, than the previously reported value (5.4 ± 0.9 fm [18]) with its large uncertainty. As was noted earlier, the present higher precision and more absorptive and surface dominated higher beam energy measurement on a nuclear (carbon) target, places the underpinning Glauber (eikonal) dynamical model description of the reaction used here on a much stronger footing regarding the magnitudes of multiple-scattering and other corrections [28,29].

Fig. 5 shows the A-dependence of $\tilde{r}_m$ for the neutron-rich carbon isotopes from the present study, where the adopted values are shown. The one-neutron halo nature of ^{19}C leads to an enhanced $\tilde{r}_m$ value relative to ^{20}C. The $\tilde{r}_m(^{22}\mathrm{C})$ is about 0.4 fm larger than that for ^{20}C, reflecting the two-neutron halo character of ^{22}C. The dashed line shows the results of an alternative mean-field model for ^{20}C and few-body models for ^{19,22}C [46]. Our deduced $\tilde{r}_m(^{22}\mathrm{C})$ is also in agreement with values: (i) ranging from 3.6–3.75 fm for $S_{2n}(^{22}\mathrm{C})$ values between 400–600 keV, of the three-body model calculation of Ref. [24], and (ii) $\tilde{r}_m(^{22}\mathrm{C}) = 3.4$ and 3.6 fm, with $S_{2n}(^{22}\mathrm{C})$ of 400 and 200 keV, of Ref. [26]. These models, like the present one, calculate an s-wave configuration of the two valence neutrons with probability $\geq 90\%$, in line with a picture in which the $N = 16$ magicity persists at ^{22}C – as suggested by other more fundamental approaches [47,48]. However, as evidenced by our analysis for ^{20}C, the reaction cross section alone is somewhat insensitive to details of the microscopic structure and more precise, more exclusive reaction experiments and mass measurements are required.

In summary, we have measured the interaction cross sections of ^{19,20,22}C on a C target at 307, 280 and 235 MeV/nucleon, respectively. Inelastic scattering of ^{20}C to bound excited states of the C target were quantified to verify the assumption that $\sigma_R \simeq \sigma_I$. The ^{22}C reaction cross section was found to be much larger than that of ^{20}C, supporting the two neutron halo nature of ^{22}C. In the case of ^{19}C, the present and previously measured σ_R (at around 950 MeV/nucleon) are consistent with the three-body reaction model calculations, and the rms radius of ^{19}C obtained was $3.10^{+0.05}_{-0.03}$ fm. For ^{20}C, occupancy of the neutron $2s_{1/2}$ orbital was needed to reproduce the present data, and the rms matter radius was estimated to be $2.97^{+0.03}_{-0.05}$ fm. The deduced ^{22}C rms matter radius, 3.44 ± 0.08 fm, from the four-body Glauber reaction model analysis, is consistent with other theoretical predictions based on ^{22}C three-body model wave functions [24,26]. The present rms radius is smaller and has a much reduced uncertainty than that of Ref. [18]. More exclusive measurements, such as Coulomb dissociation and fast neutron-knockout reactions, will allow for a more detailed study of the structure of ^{22}C, including the potential role of core excitations on the $N = 16$ magicity [49,50].

Acknowledgments

The authors thank the staff of RIKEN RIBF for their efforts in providing the ^{48}Ca beam. We are grateful to Dr. M. Takechi for discussions and providing the experimental data of Ref. [28]. The present work was supported in part by JSPS KAKENHI Grant No. 24740154, MEXT KAKENHI Grant No. 24105005, the WCU (R32-2008-000-10155-0) and the GPF (NRF-2011-0006492) programs of NRF Korea, and the HIC for FAIR. J.A.T. acknowledges support of the Science and Technology Facility Council (UK) grants ST/J000051 and ST/L005743. N.L.A., F.D., J.G., F.M.M. and N.A.O. acknowledge partial support from the Franco–Japanese LIA-International Associated Laboratory for Nuclear Structure Problems. A.N. and J.G. would also like to acknowledge the JSPS Invitation Fellowship program for long-term research in Japan at the Tokyo Institute of Technology and RIKEN respectively.

References

[1] K. Riisager, Nuclear halo states, Rev. Mod. Phys. 66 (1994) 1105.
[2] M. Matsuo, K. Mizuyama, Y. Serizawa, Di-neutron correlation and soft dipole excitation in medium mass neutron-rich nuclei near drip line, Phys. Rev. C 71 (2005) 064326.
[3] K. Hagino, H. Sagawa, J. Carbonell, P. Schuck, Coexistence of BCS- and BEC-like pair structures in halo nuclei, Phys. Rev. Lett. 99 (2007) 022506.
[4] K. Hagino, H. Sagawa, T. Nakamura, S. Shimoura, Two-particle correlations in continuum dipole transitions in Borromean nuclei, Phys. Rev. C 80 (2009) 031301.
[5] T. Myo, K. Katō, H. Toki, K. Ikeda, Roles of tensor and pairing correlations on halo formation in ^{11}Li, Phys. Rev. C 76 (2007) 024305.
[6] M. Zhukov, B. Danilin, D. Fedorov, J. Bang, I. Thompson, J. Vaagen, Bound state properties of Borromean halo nuclei: ^{6}He and ^{11}Li, Phys. Rep. 231 (4) (1993) 151.

[7] N. Shulgina, B. Jonson, M. Zhukov, ^{11}Li structure from experimental data, Nucl. Phys. A 825 (3–4) (2009) 175.

[8] B. Acharya, C. Ji, D. Phillips, Implications of a matter-radius measurement for the structure of carbon-22, Phys. Lett. B 723 (1–3) (2013) 196.

[9] T. Nakamura, A.M. Vinodkumar, T. Sugimoto, N. Aoi, H. Baba, D. Bazin, N. Fukuda, T. Gomi, H. Hasegawa, N. Imai, M. Ishihara, T. Kobayashi, Y. Kondo, T. Kubo, M. Miura, T. Motobayashi, H. Otsu, A. Saito, H. Sakurai, S. Shimoura, K. Watanabe, Y.X. Watanabe, T. Yakushiji, Y. Yanagisawa, K. Yoneda, Observation of strong low-lying $e1$ strength in the two-neutron halo nucleus ^{11}Li, Phys. Rev. Lett. 96 (2006) 252502.

[10] R. Sánchez, W. Nörtershäuser, G. Ewald, D. Albers, J. Behr, P. Bricault, B.A. Bushaw, A. Dax, J. Dilling, M. Dombsky, G.W.F. Drake, S. Götte, R. Kirchner, H.-J. Kluge, T. Kühl, J. Lassen, C.D.P. Levy, M.R. Pearson, E.J. Prime, V. Ryjkov, A. Wojtaszek, Z.-C. Yan, C. Zimmermann, Nuclear charge radii of ^{9,11}Li: the influence of halo neutrons, Phys. Rev. Lett. 96 (2006) 033002.

[11] F. Marqués, M. Labiche, N. Orr, J. Angélique, L. Axelsson, B. Benoit, U. Bergmann, M. Borge, W. Catford, S. Chappell, N. Clarke, G. Costa, N. Curtis, A. D'Arrigo, F. de Oliveira Santos, E. de Góes Brennand, O. Dorvaux, M. Freer, B. Fulton, G. Giardina, C. Gregori, S. Grévy, D. Guillemaud-Mueller, F. Hanappe, B. Heusch, B. Jonson, C.L. Brun, S. Leenhardt, M. Lewitowicz, M. López, K. Markenroth, M. Motta, A. Mueller, T. Nilsson, A. Ninane, G. Nyman, I. Piqueras, K. Riisager, M.S. Laurent, F. Sarazin, S. Singer, O. Sorlin, L. Stuttgé, Two-neutron interferometry as a probe of the nuclear halo, Phys. Lett. B 476 (3–4) (2000) 219.

[12] I. Tanihata, H. Hamagaki, O. Hashimoto, Y. Shida, N. Yoshikawa, K. Sugimoto, O. Yamakawa, T. Kobayashi, N. Takahashi, Measurements of interaction cross sections and nuclear radii in the light p-shell region, Phys. Rev. Lett. 55 (1985) 2676.

[13] T. Moriguchi, A. Ozawa, S. Ishimoto, Y. Abe, M. Fukuda, I. Hachiuma, Y. Ishibashi, Y. Ito, T. Kuboki, M. Lantz, D. Nagae, K. Namihira, D. Nishimura, T. Ohtsubo, H. Ooishi, T. Suda, H. Suzuki, T. Suzuki, M. Takechi, K. Tanaka, T. Yamaguchi, Density distributions of ^{11}Li deduced from reaction cross-section measurements, Phys. Rev. C 88 (2013) 024610.

[14] I. Tanihata, T. Kobayashi, O. Yamakawa, S. Shimoura, K. Ekuni, K. Sugimoto, N. Takahashi, T. Shimoda, H. Sato, Measurement of interaction cross sections using isotope beams of Be and B and isospin dependence of the nuclear radii, Phys. Lett. B 206 (4) (1988) 592.

[15] J.S. Al-Khalili, J.A. Tostevin, Matter radii of light halo nuclei, Phys. Rev. Lett. 76 (1996) 3903.

[16] J.S. Al-Khalili, J.A. Tostevin, I.J. Thompson, Radii of halo nuclei from cross section measurements, Phys. Rev. C 54 (1996) 1843.

[17] L. Gaudefroy, W. Mittig, N.A. Orr, S. Varet, M. Chartier, P. Roussel-Chomaz, J.P. Ebran, B. Fernández-Domínguez, G. Frémont, P. Gangnant, A. Gillibert, S. Grévy, J.F. Libin, V.A. Maslov, S. Paschalis, B. Pietras, Y.-E. Penionzhkevich, C. Spitaels, A.C.C. Villari, Direct mass measurements of ^{19}B, ^{22}C, ^{29}F, ^{31}Ne, ^{34}Na and other light exotic nuclei, Phys. Rev. Lett. 109 (2012) 202503.

[18] K. Tanaka, T. Yamaguchi, T. Suzuki, T. Ohtsubo, M. Fukuda, D. Nishimura, M. Takechi, K. Ogata, A. Ozawa, T. Izumikawa, T. Aiba, N. Aoi, H. Baba, Y. Hashizume, K. Inafuku, N. Iwasa, K. Kobayashi, M. Komuro, Y. Kondo, T. Kubo, M. Kurokawa, T. Matsuyama, S. Michimasa, T. Motobayashi, T. Nakabayashi, S. Nakajima, T. Nakamura, H. Sakurai, R. Shinoda, M. Shinohara, H. Suzuki, E. Takeshita, S. Takeuchi, Y. Togano, K. Yamada, T. Yasuno, M. Yoshitake, Observation of a large reaction cross section in the drip-line nucleus ^{22}C, Phys. Rev. Lett. 104 (2010) 062701.

[19] A. Ozawa, T. Kobayashi, T. Suzuki, K. Yoshida, I. Tanihata, New magic number, $N = 16$, near the neutron drip line, Phys. Rev. Lett. 84 (2000) 5493.

[20] M. Stanoiu, F. Azaiez, Z. Dombrádi, O. Sorlin, B.A. Brown, M. Belleguic, D. Sohler, M.G. Saint Laurent, M.J. Lopez-Jimenez, Y.E. Penionzhkevich, G. Sletten, N.L. Achouri, J.C. Angélique, F. Becker, C. Borcea, C. Bourgeois, A. Bracco, J.M. Daugas, Z. Dlouhý, C. Donzaud, J. Duprat, Z. Fülöp, D. Guillemaud-Mueller, S. Grévy, F. Ibrahim, A. Kerek, A. Krasznahorkay, M. Lewitowicz, S. Leenhardt, S. Lukyanov, P. Mayet, S. Mandal, H. van der Marel, W. Mittig, J. Mrázek, F. Negoita, F. De Oliveira-Santos, Z. Podolyák, F. Pougheon, M.G. Porquet, P. Roussel-Chomaz, H. Savajols, Y. Sobolev, C. Stodel, J. Timár, A. Yamamoto, $N = 14$ and 16 shell gaps in neutron-rich oxygen isotopes, Phys. Rev. C 69 (2004) 034312.

[21] B.A. Brown, W.A. Richter, Magic numbers in the neutron-rich oxygen isotopes, Phys. Rev. C 72 (2005) 057301.

[22] N. Kobayashi, T. Nakamura, J.A. Tostevin, Y. Kondo, N. Aoi, H. Baba, S. Deguchi, J. Gibelin, M. Ishihara, Y. Kawada, T. Kubo, T. Motobayashi, T. Ohnishi, N.A. Orr, H. Otsu, H. Sakurai, Y. Satou, E.C. Simpson, T. Sumikama, H. Takeda, M. Takechi, S. Takeuchi, K.N. Tanaka, N. Tanaka, Y. Togano, K. Yoneda, One- and two-neutron removal reactions from the most neutron-rich carbon isotopes, Phys. Rev. C 86 (2012) 054604.

[23] T. Inakura, W. Horiuchi, Y. Suzuki, T. Nakatsukasa, Mean-field analysis of ground-state and low-lying electric dipole strength in ^{22}C, Phys. Rev. C 89 (2014) 064316.

[24] W. Horiuchi, Y. Suzuki, ^{22}C: an s-wave two-neutron halo nucleus, Phys. Rev. C 74 (2006) 034311.

[25] Y. Kucuk, J.A. Tostevin, Intermediate-energy four-body breakup calculations for ^{22}C, Phys. Rev. C 89 (2014) 034607.

[26] S.N. Ershov, J.S. Vaagen, M.V. Zhukov, Binding energy constraint on matter radius and soft dipole excitations of ^{22}C, Phys. Rev. C 86 (2012) 034331.

[27] M. Yamashita, R.M. de Carvalho, T. Frederico, L. Tomio, Constraints on two-neutron separation energy in the Borromean ^{22}C nucleus, Phys. Lett. B 697 (1) (2011) 90.

[28] M. Takechi, M. Fukuda, M. Mihara, K. Tanaka, T. Chinda, T. Matsumasa, M. Nishimoto, R. Matsumiya, Y. Nakashima, H. Matsubara, K. Matsuta, T. Minamisono, T. Ohtsubo, T. Izumikawa, S. Momota, T. Suzuki, T. Yamaguchi, R. Koyama, W. Shinozaki, M. Takahashi, A. Takizawa, T. Matsuyama, S. Nakajima, K. Kobayashi, M. Hosoi, T. Suda, M. Sasaki, S. Sato, M. Kanazawa, A. Kitagawa, Reaction cross sections at intermediate energies and Fermi-motion effect, Phys. Rev. C 79 (2009) 061601.

[29] C. Bertulani, C. De Conti, Pauli blocking and medium effects in nucleon knockout reactions, Phys. Rev. C 81 (2010) 064603.

[30] I. Tanihata, H. Savajols, R. Kanungo, Recent experimental progress in nuclear halo structure studies, Prog. Part. Nucl. Phys. 68 (1) (2013) 215.

[31] T. Kubo, In-flight RI beam separator BigRIPS at RIKEN and elsewhere in Japan, Nucl. Instrum. Methods Phys. Res., Sect. B, Beam Interact. Mater. Atoms 204 (1) (2003) 97.

[32] T. Kobayashi, N. Chiga, T. Isobe, Y. Kondo, T. Kubo, K. Kusaka, T. Motobayashi, T. Nakamura, J. Ohnishi, H. Okuno, H. Otsu, T. Sako, H. Sato, Y. Shimizu, K. Sekiguchi, K. Takahashi, R. Tanaka, K. Yoneda, SAMURAI spectrometer for RI beam experiments, Nucl. Instrum. Methods Phys. Res., Sect. B, Beam Interact. Mater. Atoms 317 (1) (2013) 294.

[33] S. Takeuchi, T. Motobayashi, Y. Togano, M. Matsushita, N. Aoi, K. Demichi, H. Hasegawa, H. Murakami, Dali2: a NaI(Tl) detector array for measurements of γ rays from fast nuclei, Nucl. Instrum. Methods Phys. Res., Sect. A, Accel. Spectrom. Detect. Assoc. Equip. 763 (2014) 596.

[34] T. Yamaguchi, K. Tanaka, T. Suzuki, A. Ozawa, T. Ohtsubo, T. Aiba, N. Aoi, H. Baba, M. Fukuda, Y. Hashizume, K. Inafuku, N. Iwasa, T. Izumikawa, K. Kobayashi, M. Komuro, Y. Kondo, T. Kubo, M. Kurokawa, T. Matsuyama, S. Michimasa, T. Motobayashi, T. Nakabayashi, S. Nakajima, T. Nakamura, H. Sakurai, R. Shinoda, M. Shinohara, H. Suzuki, M. Takechi, E. Takeshita, S. Takeuchi, Y. Togano, K. Yamada, T. Yasuno, M. Yoshitake, Nuclear reactions of ^{19,20}C on a liquid hydrogen target measured with the superconducting TOF spectrometer, Nucl. Phys. A 864 (1) (2011) 1.

[35] F. Ajzenberg-Selove, Energy levels of light nuclei $A = 11$–12, Nucl. Phys. A 506 (1) (1990) 1.

[36] M. Stanoiu, D. Sohler, O. Sorlin, F. Azaiez, Z. Dombrádi, B.A. Brown, M. Belleguic, C. Borcea, C. Bourgeois, Z. Dlouhy, Z. Elekes, Z. Fülöp, S. Grévy, D. Guillemaud-Mueller, F. Ibrahim, A. Kerek, A. Krasznahorkay, M. Lewitowicz, S.M. Lukyanov, S. Mandal, J. Mrázek, F. Negoita, Y.-E. Penionzhkevich, Z. Podolyák, P. Roussel-Chomaz, M.G. Saint-Laurent, H. Savajols, G. Sletten, J. Timár, C. Timis, A. Yamamoto, Disappearance of the $N = 14$ shell gap in the carbon isotopic chain, Phys. Rev. C 78 (2008) 034315.

[37] M. Petri, P. Fallon, A.O. Macchiavelli, S. Paschalis, K. Starosta, T. Baugher, D. Bazin, L. Cartegni, R.M. Clark, H.L. Crawford, M. Cromaz, A. Dewald, A. Gade, G.F. Grinyer, S. Gros, M. Hackstein, H.B. Jeppesen, I.Y. Lee, S. McDaniel, D. Miller, M.M. Rajabali, A. Ratkiewicz, W. Rother, P. Voss, K.A. Walsh, D. Weisshaar, M. Wiedeking, B.A. Brown, Lifetime measurement of the 2_1^+ state in ^{20}C, Phys. Rev. Lett. 107 (2011) 102501.

[38] M. Takechi, S. Suzuki, D. Nishimura, M. Fukuda, T. Ohtsubo, M. Nagashima, T. Suzuki, T. Yamaguchi, A. Ozawa, T. Moriguchi, H. Ohishi, T. Sumikama, H. Geissel, N. Aoi, R.-J. Chen, D.-Q. Fang, N. Fukuda, S. Fukuoka, H. Furuki, N. Inabe, Y. Ishibashi, T. Itoh, T. Izumikawa, D. Kameda, T. Kubo, M. Lantz, C.S. Lee, Y.-G. Ma, K. Matsuta, M. Mihara, S. Momota, D. Nagae, R. Nishikiori, T. Niwa, T. Ohnishi, K. Okumura, M. Ohtake, T. Ogura, H. Sakurai, K. Sato, Y. Shimbara, H. Suzuki, H. Takeda, S. Takeuchi, K. Tanaka, M. Tanaka, H. Uenishi, M. Winkler, Y. Yanagisawa, S. Watanabe, K. Minomo, S. Tagami, M. Shimada, M. Kimura, T. Matsumoto, Y.R. Shimizu, M. Yahiro, Evidence of halo structure in ^{37}Mg observed via reaction cross sections and intruder orbitals beyond the island of inversion, Phys. Rev. C 90 (2014) 061305.

[39] A. Ozawa, O. Bochkarev, L. Chulkov, D. Cortina, H. Geissel, M. Hellström, M. Ivanov, R. Janik, K. Kimura, T. Kobayashi, A. Korsheninnikov, G. Münzenberg, F. Nickel, Y. Ogawa, A. Ogloblin, M. Pfützner, V. Pribora, H. Simon, B. Sitár, P. Strmen, K. Sümmerer, T. Suzuki, I. Tanihata, M. Winkler, K. Yoshida, Measurements of interaction cross sections for light neutron-rich nuclei at relativistic energies and determination of effective matter radii, Nucl. Phys. A 691 (3–4) (2001) 599.

[40] S. Kox, A. Gamp, C. Perrin, J. Arvieux, R. Bertholet, J. Bruandet, M. Buenerd, Y.E. Masri, N. Longequeue, F. Merchez, Transparency effects in heavy-ion collisions over the energy range 100–300 MeV/nucleon, Phys. Lett. B 159 (1) (1985) 15.

[41] B.A. Brown, New Skyrme interaction for normal and exotic nuclei, Phys. Rev. C 58 (1998) 220.

[42] L. Ray, Proton–nucleus total cross sections in the intermediate energy range, Phys. Rev. C 20 (1979) 1857.

[43] G. Audi, M. Wang, A. Wapstra, F. Kondev, M. MacCormick, X. Xu, B. Pfeiffer, The Ame2012 atomic mass evaluation, Chin. Phys. C 36 (12) (2012) 1287.

[44] B. Buck, A. Pilt, Alpha-particle and triton cluster states in ^{19}F, Nucl. Phys. A 280 (1) (1977) 133.

[45] Y. Yamaguchi, C. Wu, T. Suzuki, A. Ozawa, D.Q. Fang, M. Fukuda, N. Iwasa, T. Izumikawa, H. Jeppesen, R. Kanungo, R. Koyama, T. Ohnishi, T. Ohtsubo, W. Shinozaki, T. Suda, M. Takahashi, I. Tanihata, Density distribution of ^{17}B from a reaction cross-section measurement, Phys. Rev. C 70 (2004) 054320.
[46] B. Abu-Ibrahim, W. Horiuchi, A. Kohama, Y. Suzuki, Reaction cross sections of carbon isotopes incident on a proton, Phys. Rev. C 77 (2008) 034607.
[47] L. Coraggio, A. Covello, A. Gargano, N. Itaco, Shell-model calculations for neutron-rich carbon isotopes with a chiral nucleon–nucleon potential, Phys. Rev. C 81 (2010) 064303.
[48] G.R. Jansen, J. Engel, G. Hagen, P. Navratil, A. Signoracci, *Ab initio* coupled-cluster effective interactions for the shell model: application to neutron-rich oxygen and carbon isotopes, Phys. Rev. Lett. 113 (2014) 142502.
[49] T. Suzuki, T. Otsuka, C. Yuan, A. Navin, Two-neutron halo from the low-energy limit of neutron–neutron interaction: applications to drip-line nuclei ^{22}C and ^{24}O, Phys. Lett. B 753 (2016) 199.
[50] K. Ogata, T. Myo, T. Furumoto, T. Matsumoto, M. Yahiro, Interplay between the 0_2^+ resonance and the nonresonant continuum of the drip-line two-neutron halo nucleus ^{22}C, Phys. Rev. C 88 (2013) 024616.